

# Optimal Smart Home Energy Management Considering Energy Saving and a Comfortable Lifestyle

Amjad Anvari-Moghaddam, *Graduate Student Member, IEEE*, Hassan Monsef, and  
Ashkan Rahimi-Kian, *Senior Member, IEEE*

**Abstract**—One of the most challenging problems associated with operation of smart micro-grids is the optimal energy management of residential buildings with respect to multiple and often conflicting objectives. In this paper, a multiobjective mixed integer nonlinear programming model is developed for optimal energy use in a smart home, considering a meaningful balance between energy saving and a comfortable lifestyle. Thorough incorporation of a mixed objective function under different system constraints and user preferences, the proposed algorithm could not only reduce the domestic energy usage and utility bills, but also ensure an optimal task scheduling and a thermal comfort zone for the inhabitants. To verify the efficiency and robustness of the proposed algorithm, a number of simulations were performed under different scenarios using real data, and the obtained results were compared in terms of total energy consumption cost, users' convenience rates, and thermal comfort level.

**Index Terms**—Demand response, energy management system, micro-grid, smart home, thermal comfort zone.

## I. INTRODUCTION

THE PRESENT and future smart grids play important roles in delivery of electricity from suppliers to industrial, commercial, and residential zones in an efficient, reliable, and secure manner. With the aid of such intelligent grids in micro/macro scales, not only the wasteful use of energy for householders and business owners would be decreased, but also further utilization of renewable energy sources will be provided. Regarding a smart micro-grid (SMG), two-way digital communications between the utility and common household devices could be enabled through the joint operation of smart energy management systems and advanced smart grid components, giving the users tools to improve their energy efficiency and to participate in programs such as time-of-day pricing for lowering their costs of energy consumption [1]. Since buildings contribute to a major portion of overall electricity consumption, many researchers around the world

have elaborated on demand-side energy management problem and have proposed a large number of power scheduling schemes both in domestic and residential sectors [2]–[12]. As an example, Molderink *et al.* [2] presented a domestic energy management methodology based on the optimal switching of thermal appliances to minimize energy consumption costs, while considering thermal constraints. In a similar way, Mohsenian-Rad and Leon-Garcia [3] proposed an optimization algorithm for minimization of users' electricity bills considering their comfort levels as the problem constraints. Although the authors introduced the waiting time ranges as measures of the user's comfort, they failed to model the behaviors of different home appliances. Mohsenian-Rad *et al.* [4] proposed a game-based approach for optimal energy management of a residential building and justified the goodness of the global state by giving some reasons, but they failed to consider the user's satisfaction degree as an objective for efficient task scheduling. Optimal scheduling of in-home appliances with storage device buffering has been also presented in [5] considering the total cost minimization as the objective of the optimization problem. Likewise, an appliance commitment algorithm for household load scheduling has been introduced in [6] considering the minimum electricity consumption cost as the only objective. Beyond what has been stated in the field of demand-side management in smart grids, there exist numerous techniques in recent works, which have been applied for domestic energy management and task scheduling aims [7]–[12]. Although these techniques have been mainly based on deterministic and/or meta-heuristic methods, they have failed to consider the users' convenience and comfort levels as competitive objectives in their optimization problems.

To the best of our knowledge, none of the previous research works have considered a detailed optimization problem, which has taken into account the energy saving and comfortable lifestyle as objectives of a realistic smart home energy management system. Therefore in this paper, a multiobjective mixed integer nonlinear programming (MO-MINLP) model is developed for optimal energy use in a home considering energy saving, user's convenience rate and thermal comfort level (TCL) as three dependent objectives. Moreover, a composite architecture for home energy management system is presented, where each in-home device can be modeled as a collection of functions that represent its behavior.

Manuscript received March 3, 2014; revised June 3, 2014; accepted July 8, 2014. This work was supported in part by the Research Center of Power System Operation and Planning Studies; and in part by the Smart Networks Laboratory/Center of Excellence for Control and Intelligent Processing, School of Electrical and Computer Engineering, College of Engineering, University of Tehran, Tehran, Iran. Paper no. TSG-00194-2014.

The authors are with the School of Electrical and Computer Engineering, College of Engineering, University of Tehran, Tehran 14395/515, Iran (e-mail: a.anvari@ut.ac.ir; hmonsef@ut.ac.ir; arkian@ut.ac.ir).

Digital Object Identifier 10.1109/TSG.2014.2349352

The main contributions of this paper could be summarized as follows.

- 1) Joint scheduling and operation management of different household devices and energy supply options is presented with regard to a new mixed objective function.
- 2) User's satisfaction degrees and comfort levels both in thermal and electrical zones are formulated and evaluated.
- 3) The overall energy management optimization framework has been improved from a thermal view point through introduction of different sources of heat generation and various heat flows.

The rest of the paper is organized as follows. A brief description of home automation/energy management system (HAEMS) is presented in Section II. Section III deals with optimal home energy scheduling and its problem formulation. The case studies and simulation results are provided in Section IV, whereas Section V draws the conclusion and future works.

## II. HAEMS

Intelligent HAEMS is the key component of the future smart homes that benefits from several communication domains, including the smart meter domain (AMI), the internet domain, and home area network (HAN) [13]. Generally, a HAEMS receives information about task operating status, usage requests, and network signals and sends control actions back to the smart devices. It is a system that provides useful feedbacks about consumption habits to the occupants, while making control decisions autonomously. It uses information about the home's environment and operation in order to identify solutions for different user's objectives such as energy saving and a comfortable lifestyle. In other words, the task of a HAEMS is to produce an optimal solution for the weighted combination of objectives over a time horizon based on a series of user's inputs and control actions.

## III. OPTIMAL HOME ENERGY SCHEDULING

### A. System Description

In this paper, the case study includes a modern medium size house in a residential micro-grid with a HAEMS and a collection of schedulable devices that control the amount of energy consumed (or produced) in the house over discrete time steps ( $\Delta h_{\text{step}} = 1$  h) with regard to residents' comfort levels and energy consumption costs. The required thermal/electric energy is provided both by the utility and internal energy sources such as micro cogeneration systems and underfloor heating/cooling units. The surplus of electrical energy could be stored in batteries, while extra thermal energy could be saved inside the tank in the form of hot water. Through the use of smart meter, the HAEMS supports net metering, gets real-time electricity price, and other input parameters (such as outdoor temperature and devices requests) and defines the optimal operation of in-home devices and demand response actions in every decision period considering the user's preferences, devices' constraints and total power limits in the house.

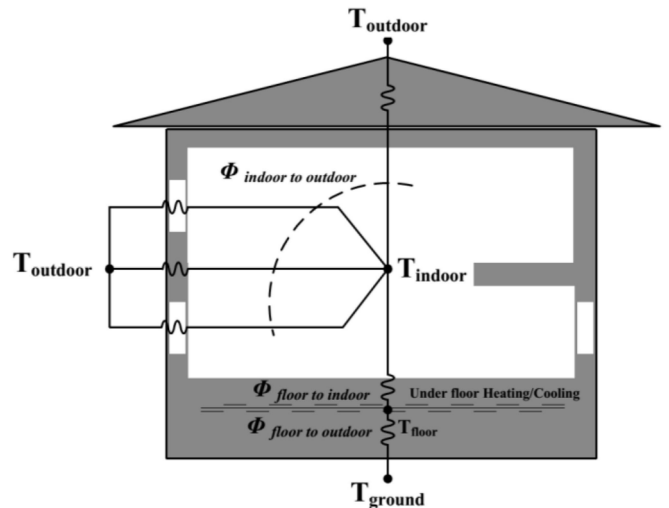


Fig. 1. Thermal modeling of a building.

### B. Problem Formulation

The mathematical modeling of the aforementioned HAEMS system is presented as follows.

### C. House Thermal Model

When developing strategies to minimize the energy consumptions within a building, it is crucial to understand the sources of energy generation and losses. Considering an under-floor heating/cooling system as the one shown in Fig. 1, the heat can transfer through different paths: between the indoor air node and the outdoor environment ( $\phi_{ao}$ ) through thermal resistance  $R_{ao}$ , between the floor and the indoor air ( $\phi_{fa}$ ) through thermal resistance  $R_{fa}$ , and finally between the floor and the ground ( $\phi_{fg}$ ) through thermal resistance  $R_{fg}$ . Based on a simple lumped model, the thermal resistance across a layer of area ( $A$ ), thickness ( $x$ ), and thermal conductivity ( $k$ ) is defined as [14], [15]

$$R_{\text{layer}} = \frac{x}{k \cdot A} = \frac{R_{\text{value}}}{A}. \quad (1)$$

Once the thermal resistances are defined, the mentioned heat flows could be calculated as follows:

$$\phi_{ao}(h) = (T_{\text{indoor}}(h) - T_{\text{outdoor}}(h)) / R_{ao} \quad (2)$$

$$\phi_{fa}(h) = (T_{\text{floor}}(h) - T_{\text{indoor}}(h)) / R_{fa} \quad (3)$$

$$\begin{aligned} \phi_{fg}(h) &= (T_{\text{floor}}(h) - T_{\text{ground}}(h)) / R_{fg} \\ &\cong (T_{\text{floor}}(h) - T_{\text{outdoor}}(h)) / R_{fg} \end{aligned} \quad (4)$$

where,  $T_{\text{indoor}}(h)$ ,  $T_{\text{outdoor}}(h)$ , and  $T_{\text{ground}}(h)$  are the temperatures of indoor air, outdoor environment, and the ground at hour  $h$ . In the above formulation, the assumption of  $T_{\text{ground}} \equiv T_{\text{outdoor}}$  would also be fair due to the ventilated crawl space in the house. In addition to heat transfers and losses, one should also determine the sources of heat generation within a building. In this paper, these sources mainly include the buildings' heating/cooling system, solar radiation, occupants' metabolisms, and the effect of background electric appliances. Although wind speed is regarded as another important factor

that increases heat transfer to or from the building by increasing the infiltration and the convection heat transfer coefficient, its effect is neglected in this paper.

As the main source of thermal energy, the assumed heating/cooling system includes a heat pump, which heats up (or cools down) the water and pumps it through the piping embedded inside the floor of the house. In this regard, the amount of thermal energy that is supplied to the floor of the house ( $\phi_{HCS}$ ) is determined as follows:

$$\phi_{HCS}(h) = \left( \frac{u_{HCS}(h) \cdot \eta_H(h) - (1 - u_{HCS}(h)) \cdot \eta_C(h)}{1} \right) P_{HCS}(h) \quad (5)$$

$$0 \leq P_{HCS}(h) \leq P_{HCS,max} \quad (6)$$

$$\eta_{H,min} \leq \eta_H(h) \leq \eta_{H,max} \quad (7)$$

$$\eta_{C,min} \leq \eta_C(h) \leq \eta_{C,max} \quad (8)$$

where,  $u_{HCS}$  is a binary showing the system's operation status ("1" = Heating, "0" = Cooling), and  $P_{HCS}(h)$  is the power consumption of the heat pump at hour  $h$  limited by its upper bound  $P_{HCS,max}$ ;  $\eta_H(\eta_C)$  is the heating (cooling) coefficient of the performance (COP), which is roughly a linear function of the outdoor temperature and is calculated as follows [15]:

$$\eta_H(h) = \begin{cases} \eta_{H,min} & ; t_{outdoor}(h) \leq \Delta t_{HO} \\ \frac{\eta_{H,max} - \eta_{H,min}}{t_H - \Delta t_{HO}} (t_{outdoor}(h) - \Delta t_{HO}) + \eta_{H,min} & ; \Delta t_{HO} \leq t_{outdoor}(h) \leq t_H \\ \eta_{H,max} & ; t_{outdoor}(h) \geq t_H \end{cases} \quad (9)$$

$$\eta_C(h) = \begin{cases} \eta_{C,min} & ; t_{outdoor}(h) \geq \Delta t_{CO} \\ \frac{\eta_{C,min} - \eta_{C,max}}{t_C - \Delta t_{CO}} (t_{outdoor}(h) - \Delta t_{CO}) + \eta_{C,min} & ; t_C \leq t_{outdoor}(h) \leq \Delta t_{CO} \\ \eta_{C,max} & ; t_{outdoor}(h) \leq t_C \end{cases} \quad (10)$$

where,  $t_H(t_C)$  is the temperature of fluid that flows under the floor when heating (cooling) and  $\Delta t_{HO}(\Delta t_{CO})$  is the temperature difference between  $t_H(t_C)$  and the outdoor temperature. Similarly,  $\eta_{H,min}(\eta_{C,min})$  and  $\eta_{H,max}(\eta_{C,max})$  are the theoretical lower and upper bounds of heating (cooling) COP, respectively.

Solar radiation, as the second energy source, plays a major role on the heating/cooling of a building. Since solar radiation enters the house through the windows directly, and is absorbed by the walls and the roof (which is released later in the day), it has a considerable effect on the peak cooling load of a building. In this regard, as shown in Fig. 2, the hourly heat flow into an exterior surface of a building subjected to solar radiation can be expressed as

$$\begin{aligned} \phi_{surface}(h) &= \phi_{conv}(h) + \phi_{solar}(h) - \phi_{radiation \text{ correction}}(h) \\ &= h_o A_s (T_{outdoor}(h) - T_{surface}(h)) + \alpha_s A_s \phi_{solar}(h) \\ &\quad - \varepsilon A_s \sigma (T_{outdoor}^4(h) - T_{surr}^4(h)) \\ &= h_o A_s (T_{eq\_out}(h) - T_{surface}(h)) \end{aligned} \quad (11)$$

where,  $h_o$  is the combined convection and radiation heat transfer coefficient in  $W/(m^2.K)$ ,  $\alpha_s$  is the solar absorptivity and  $\varepsilon$  is the emissivity of the surface,  $\phi_{solar}$  is the solar radiation incident on the surface in  $W/m^2$ , and  $\sigma$  is Stefan-Boltzmann constant [=  $5.67 \times 10^{-8} W/(m^2.K^4)$ ]. The first term on the

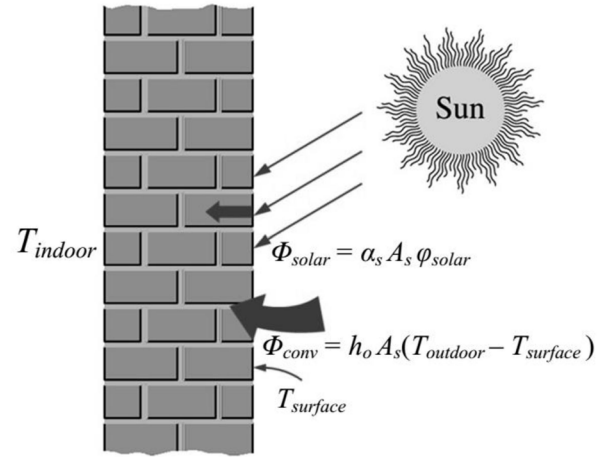


Fig. 2. Solar radiation effect on heating and cooling of a building.

right-hand side of (11) represents the convection and radiation heat transfer to the surface when the average surrounding surface and sky temperature are equal to the outdoor air temperature ( $T_{surr} = T_{outdoor}$ ) and the last term represents the correction for the radiation heat transfer when  $T_{surr} \neq T_{outdoor}$ . Equation (10) can be written as

$$T_{eq\_out}(h) = T_{outdoor}(h) + \frac{\alpha_s \phi_{solar}(h)}{h_o} - \frac{\varepsilon \sigma (T_{outdoor}^4(h) - T_{surr}^4(h))}{h_o} \quad (12)$$

where,  $T_{eq\_out}$  is the equivalent outdoor air temperature due to the solar radiation effect. Once  $T_{eq\_out}$  is available, the heat transfer through an exterior surface (such as a wall or a roof) into the indoor environment could be expressed as follows:

$$\begin{aligned} \phi_{sa}(h) &= U A_s (T_{eq\_out}(h) - T_{indoor}(h)) \\ &= \frac{T_{eq\_out}(h) - T_{indoor}(h)}{R_{sa}} \end{aligned} \quad (13)$$

In (13),  $U$  and  $R_{sa}$  are the overall heat transfer coefficient and thermal resistivity of the exposed surface, respectively, and  $A_s$  is the surface area.

Similar to other sources of thermal energy, the heat given off by the occupants' metabolisms, lights, appliances, and miscellaneous equipment such as computers, contribute to the internal heating of a building. Although such a heat gain differs during various users' activities, its average amount could be determined from the people's lifestyle. Putting all the mentioned thermal models into a nutshell, the temperature state functions of a given house could be determined as follows:

$$\begin{aligned} T_{floor}(h) &= T_{floor}(h-1) \\ &\quad + \frac{\Delta h_{step}}{m_f c_{p,f}} (\phi_{HCS}(h) + \phi_{sf}(h) - \phi_{fg}(h) - \phi_{fa}(h)) \end{aligned} \quad (14)$$

$$\begin{aligned} T_{indoor}(h) &= T_{indoor}(h-1) \\ &\quad + \frac{\Delta h_{step}}{m_a c_{p,a}} (\phi_{fa}(h) + \phi_{sa}(h) + \phi_{ihg}(h) - \phi_{ao}(h)) \end{aligned} \quad (15)$$

where,  $m_f$ ,  $m_a$ ,  $c_{p,f}$ , and  $c_{p,a}$  are the mass and specific heat capacity coefficients of the floor and air, respectively;  $\phi_{\text{ing}}(h)$  is the internal heat gain of the building from the occupants' metabolisms and other home appliances at hour  $h$ , and  $\phi_{\text{st}}(h)$  is the heat obtained directly from solar radiation when it enters the house through the windows; and is absorbed by the floor area ( $A_f$ ) with solar absorptivity of  $\alpha_f$ . Without loss of generality,  $\phi_{\text{st}}(h)$  can be stated as follows:

$$\phi_{\text{st}}(h) = \alpha_f \cdot \phi_{\text{solar}}(h) \cdot A_f. \quad (16)$$

#### D. Fuel Cell Cogeneration System

In this paper, a micro-combined heat and power system (micro-CHP) composed of a water tank, a backup boiler, and a fuel cell (FC) unit is considered as a residential cogeneration system to serve the home's hot water needs and provide unmet electrical demand through its cost-effective operation. In a FC-based micro-CHP system, the FC unit converts natural gas  $G_{\text{FC}}$  into electricity  $P_{\text{CHP}}^e$  and heat  $P_{\text{CHP}}^{\text{th}}$  as follows:

$$P_{\text{CHP}}^e(h) = \frac{G_{\text{FC}}(h)}{G_{\text{ref}}} \cdot \eta_e = P_{\text{CHP}}^{\text{th}}(h) \cdot \frac{\eta_e}{\eta_{\text{th}}} \quad (17)$$

where,  $G_{\text{ref}}$  is the natural gas consumption rate of a CHP system for producing 1 kWh energy and  $\eta_e$  and  $\eta_{\text{th}}$  are the electric and thermal efficiencies of the FC unit, respectively. The electrical and thermal power outputs of a micro-CHP unit are constrained by certain minimum and maximum capacities as well as ramp rates modeled as follows:

$$u_{\text{CHP}}(h) \cdot P_{\text{CHP}, \min}^e \leq P_{\text{CHP}}^e(h) \leq u_{\text{CHP}}(h) \cdot P_{\text{CHP}, \max}^e \quad (18)$$

$$u_{\text{CHP}}(h) \cdot P_{\text{CHP}, \min}^{\text{th}} \leq P_{\text{CHP}}^{\text{th}}(h) \leq u_{\text{CHP}}(h) \cdot P_{\text{CHP}, \max}^{\text{th}} \quad (19)$$

$$|P_{\text{CHP}}^e(h) - P_{\text{CHP}}^e(h-1)| \leq P_{\text{CHP}, \text{ramp}}^e. \quad (20)$$

The same constraints must also be satisfied for the backup (auxiliary) boiler

$$\begin{aligned} u_{\text{aux}}(h) \cdot P_{\text{aux}, \min}^{\text{th}} &\leq \left( P_{\text{aux}}^{\text{th}}(h) = \frac{G_{\text{aux}}(h)}{G_{\text{ref}}} \cdot \eta_{\text{aux}} \right) \\ &\leq u_{\text{aux}}(h) \cdot P_{\text{aux}, \max}^{\text{th}} \end{aligned} \quad (21)$$

where,  $P_{\text{aux}, \min}^{\text{th}}$  and  $P_{\text{aux}, \max}^{\text{th}}$  are the minimum and maximum heat outputs of the auxiliary boiler,  $\eta_{\text{aux}}$  is the boiler efficiency and  $G_{\text{aux}}(h)$  is the total gas flow to the backup system at hour  $h$ . The binary variables  $u_{\text{CHP}}$  and  $u_{\text{aux}}$  also denote the on ("1") or off ("0") states of the corresponding units. If the interaction of available hot water in the system tank and the cold water from the water inlet is considered, the energy storage content  $Q_{\text{st}}(h)$  can be updated at each time step as

$$Q_{\text{st}}(h+1) = Q_{\text{st}}(h) + \left( \frac{P_{\text{CHP}}^{\text{th}}(h) + P_{\text{aux}}^{\text{th}}(h) - P_{\text{demand}}^{\text{th}}(h) - P_{\text{loss}}^{\text{th}}(h)}{V_{\text{tot}}} \right) \cdot \Delta h_{\text{step}} \quad (22)$$

where,  $P_{\text{demand}}^{\text{th}}(h)$  and  $P_{\text{loss}}^{\text{th}}(h)$  are the heat demand and heat loss of the hot water storage at hour  $h$ , respectively. Likewise, the water storage temperature at each hour ( $T_{\text{st}}(h)$ ) could be updated according to the following equations:

$$\begin{aligned} T_{\text{st}}(h+1) &= \frac{V_{\text{demand}}^{\text{th}}(h) \cdot (T_{\text{cw}} - T_{\text{st}}(h)) + V_{\text{tot}} \cdot T_{\text{st}}(h)}{V_{\text{tot}}} \\ &+ \frac{P_{\text{CHP}}^{\text{th}}(h) + P_{\text{aux}}^{\text{th}}(h)}{V_{\text{tot}} \cdot C_w} - \frac{A_{\text{st}}}{R_{\text{st}}} (T_{\text{st}}(h) - T_b(h)) \end{aligned} \quad (23)$$

$$T_{\text{st}, \min} \leq T_{\text{st}}(h) \leq T_{\text{st}, \max} \quad (24)$$

where,  $V_{\text{tot}}$  and  $V_{\text{demand}}^{\text{th}}(h)$  are the total storage volume and hourly occupants' hot water demand in liter, and  $T_{\text{cw}}$  and  $T_b(h)$  are the entering cold water and the basement temperatures, respectively. The last term on the right side of (23) refers to the thermal losses of the tank (to the environment), which greatly depends on the surface area of the tank ( $A_{\text{st}}$ ),  $R$ -value of the insulation material ( $R_{\text{st}}$ ), and the temperature difference between the hot water and the basement.

#### E. Energy Storage Device

A modern household in a SMG is expected to be equipped with some form of energy storage/production devices such as batteries or plug-in hybrid electric vehicles (PHEVs). To keep high battery efficiency, the charging/discharging power and the state-of-charge (SoC) should be constrained within certain ranges as follows:

$$P_{\text{Batt}, \text{ch}}(h) \leq P_{\text{ch}, \max} \cdot \eta_{\text{ch}} \cdot u_{\text{Batt}}(h) \quad (25)$$

$$P_{\text{Batt}, \text{dch}}(h) \leq \left( \frac{P_{\text{dch}, \max}}{\eta_{\text{dch}}} \right) \cdot (1 - u_{\text{Batt}}(h)) \quad (26)$$

$$\text{SoC}_{\min} \leq \text{SoC}(h) \leq \text{SoC}_{\max} \quad (27)$$

where,  $P_{\text{ch}, \max}$  and  $P_{\text{dch}, \max}$  are the battery maximum charging and discharging powers and  $\text{SoC}_{\min}$  and  $\text{SoC}_{\max}$  are the lower and upper bounds of the battery's SoC, respectively. In a similar manner,  $\eta_{\text{ch}}$  and  $\eta_{\text{dch}}$  are the battery's charging and discharging efficiencies, and  $u_{\text{Batt}}(h)$  is a binary variable that shows the battery's status at hour  $h$  ("1" = charging and "0" = discharging). Considering the above constraints, the SoC update function is given by

$$\text{SoC}(h+1) = \text{SoC}(h) + \frac{(P_{\text{Batt}, \text{ch}}(h) - P_{\text{Batt}, \text{dch}}(h)) \cdot \Delta h_{\text{setp}}}{E_{\text{Batt}}} \quad (28)$$

where,  $E_{\text{Batt}}$  is the battery capacity in kWh. Although a PHEV is essentially the same as the battery, a few additional constraints such as the trip signal (showing that the PHEV battery could only be charged/discharged when it is at home) and hourly  $\text{SoC}_{\min}$  (showing that minimum energy of the PHEV battery) must be satisfied as well.

#### F. Schedulable Tasks and Residential Load Model

Residential loads generally fall into two categories: 1) schedulable loads (shiftable and curtailable tasks); and 2) fixed loads. While loads such as refrigerator and stove are regarded as fixed ones, the space heating and cooling, vacuum cleaner, washer, and dryer are examples of schedulable tasks that use most of the electricity in a household and have different behaviors in response to changes in the price of electricity over time [16]. With a focus on shiftable loads, there exists several parameters that should be set by the residents for efficient scheduling, including the utilization time range ( $\text{UTR}_i = [h_{s,i}, h_{f,i}]$ ) during which, task  $i$  is valid for scheduling; the preferred time range ( $\text{PTR}_i = [h_{e,i}, h_{l,i}]$ ) during which, task  $i$  is better to be scheduled according to the user's preferences; the length of operation time ( $\text{LOT}_i$ ), and the estimated energy

consumption ( $EEC_i$ ). Through these definitions, the power consumption of shiftable task  $i$  at hour  $h$  would be

$$P_{Dschd,i}(h) = \frac{EEC_i}{LOT_i} \cdot s_i(h); \quad \forall (h \in UTR_i, i \in N) \quad (29)$$

where,  $s_i(h)$  is a binary value with “1” for task  $i$  scheduling and “0” for task  $i$  dropping. For each task, from the set of schedulable tasks  $N$ , there are also several constraints that must be met suitably: first, task  $i$  must be completed before the end of optimization time  $h_{f,i}$

$$\sum_{h=h_{s,i}}^{h_{f,i}} s_i(h) = LOT_i. \quad (30)$$

Second, some tasks need to run once within a time window and should not be turned off before the completion

$$\sum_{h=h_{s,i}}^{h_{f,i}} |s_i(h) - s_i(h-1)| \leq 2. \quad (31)$$

Third, one task (e.g., task  $j$ ) may depend on the completion of another task (e.g., task  $i$ )

$$\sum_{h=h_{s,j}}^{h_{f,j}} s_j(h) \cdot H\left(\lambda - LOT_i + \sum_{\hat{h}=h_s}^h s_i(\hat{h})\right) = LOT_j \quad (32)$$

where,  $h_s = \min(h_{s,i}, h_{s,j})$ ,  $\lambda$  is a positive number smaller than 1 and  $H(\cdot)$  denotes a Heaviside step function. It is worth to note that the scheduling status of any given task is set to zero out of its utilization time range.

Fourth, if a large time gap between the operations of two consecutive tasks is not desired, the following constraint must be considered as well:

$$\begin{aligned} & Ord(\hat{h}) \cdot H(s_j(\hat{h}) - s_j(\hat{h}-1) - \lambda) \\ & \leq (Ord(h) - 1) \cdot H(s_i(h-1) - s_i(h) - \lambda) \\ & + \Lambda_{i,j}; \quad \forall (h \in UTR_i, \hat{h} \in UTR_j) \end{aligned} \quad (33)$$

in which,  $Ord(\cdot)$  is a function that returns the relative position of a member in a given set and  $\Lambda_{i,j}$  is the maximum allowed time gap between the operations of two consecutive tasks  $i$  and  $j$ . In addition to the aforementioned constraints, there exists a common constraint for the maximum allowable power consumption of a house ( $P_{House}^{\max}$ ) as follows:

$$P_D(h) = P_{Dfix}(h) + \sum_{i=1}^N P_{Dschd,i}(h) \leq P_{House}^{\max}. \quad (34)$$

### G. Objective Functions

*Objective 1:* Minimization of the total operation cost.

The total cost of operation in short-term for a typical house includes the costs of power exchange with the utility and the fuel cost of cogeneration system

$$\begin{aligned} & \text{Min : Cost} \\ & = \sum_{h=1}^T \left( \begin{aligned} & \rho_{grid}(h) \cdot P_{grid}(h) \\ & + \rho_{gas} \cdot (u_{CHP}(h) \cdot G_{FC}(h) + u_{aux}(h) \cdot G_{aux}(h)) \\ & + S_{CHP} |u_{CHP}(h) - u_{CHP}(h-1)| \end{aligned} \right) \end{aligned} \quad (35)$$

where,  $\rho_{grid}(h)$  and  $P_{grid}(h)$  are the real-time electricity price

and the amount of power bought (or sold) from (or to) the utility at hour  $h$ , respectively;  $\rho_{gas}$  is the natural gas price in cent per cubic meter, and  $G_{FC}(h)$  and  $G_{aux}(h)$  are the total amount of gas consumed by the FC unit and the auxiliary boiler at hour  $h$ , respectively. To avoid intermittent operation of a micro-CHP system and meet the thermal load continuously, the start-up/shut-down cost ( $S_{CHP}$ ) is also introduced for such a system.

*Objective 2:* Maximization of the user’s convenience level (UCL).

As mentioned beforehand, all schedulable tasks in a home have their own utilization and PTRs, which can be used as measurement tools for the UCL and the satisfaction of the users could be obtained when those tasks are executed at different times. To include the user’s satisfaction level as an objective function, the following formulation could be introduced:

$$\text{Max : UCL} = \sum_{i=1}^N w_i \cdot CV_i(h) \quad (36)$$

where,  $w_n \in \{1,2,3\}$  is the weight coefficient reflecting the significance of task  $i$  from the lowest priority “1” to highest one “3,” and  $CV_i(h)$  is the user’s convenience value when task  $i$  is executed at hour  $h$

$$CV_i(h) = \begin{cases} 1; & h \in PTR_i \\ \left( \begin{aligned} & H(h_{e,i} - h) \cdot (\alpha_e \cdot \exp(h - h_{e,i})) \\ & + H(h - h_{l,i}) \cdot (\alpha_l \cdot \exp(h_{l,i} - h)) \end{aligned} \right); & Oth \end{cases} \quad (37)$$

where,  $\alpha_e, \alpha_l \in R^+$  are the leading coefficients of the natural exponential functions used for controlling the penalty values over the optimization process, and  $H(\cdot)$  is a Heaviside step function.

*Objective 3:* Maximization of the TCL.

From a heating/cooling viewpoint, a user’s comfort mainly depends on three environmental factors including the temperature, relative humidity, and the air motion among which the indoor temperature is the most important one. Moreover, according to the extensive research works on human’s thermal comfort zone, it has been observed that most of normally clothed people (resting or doing light work) feel comfortable in the operative temperature range of 23–27 °C [14]. Considering the above statements, the TCL for a human body could be described as follows:

$$\text{Max : TCL} = \sum_{h=1}^T CL_{th}(h) \quad (38)$$

where,  $CL_{th}(h)$  represents the level of thermal comfort experienced by the inhabitants at each time step and is formulated as

$$CL_{th}(h) = \begin{cases} \beta_c \cdot \exp(T_{indoor}(h) - T_{set} + \Delta T_{ther}) & ; T_{indoor}(h) - T_{set} < -\Delta T_{ther} \\ 1 & ; |T_{indoor}(h) - T_{set}| \leq \Delta T_{ther} \\ \beta_h \cdot \exp(T_{set} + \Delta T_{ther} - T_{indoor}(h)) & ; T_{indoor}(h) - T_{set} > +\Delta T_{ther} \end{cases} \quad (39)$$

where,  $T_{set}$  is the user-specified set point for indoor temperature and  $\Delta T_{ther}$  is the threshold temperature difference.  $\beta_c, \beta_h \in R^+$  are also the leading coefficients of the natural

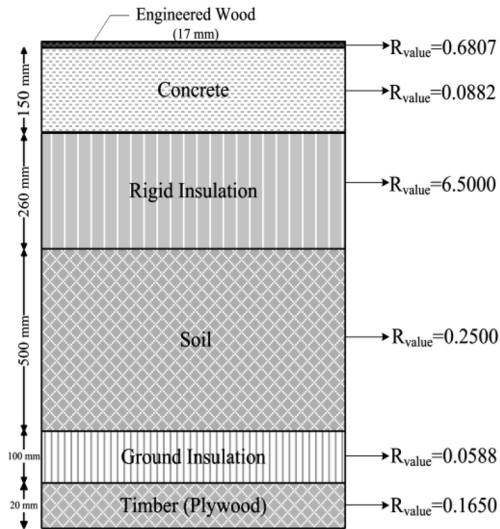


Fig. 3. Structural layers of the floor.

exponential functions used for adjusting the penalty values assigned to the undesirable lower and higher temperature differences, respectively.

#### H. Optimization Model

Since optimal energy management of a residential building inherently involves multiple, conflicting, and incommensurate objectives as mentioned before, a mixed objective function is proposed as the model of optimization

$$\text{Min} : J = \frac{\text{Cost}}{\xi_1 \cdot \text{UCL} + \xi_2 \cdot \text{TCL}} \quad (40)$$

where,  $\xi_{1,2} \in [0, 1]$ ,  $\xi_1 + \xi_2 = 1$  are the weighting coefficients determined by the residents and represent the significance of individual objectives shown in (36) and (38), respectively. The above mixed objective function must be optimized subject to the following demand-supply balance equation and all the previously mentioned constraints for the considered problem:

$$P_{\text{grid}}(h) + P_{\text{CHP}}^e(h) - (P_{\text{Batt, ch}}(h) - P_{\text{Batt, dch}}(h)) = P_D(h). \quad (41)$$

#### IV. SIMULATION RESULTS

For the simulation studies, one of the variations of a real single-zone, low-energy house in Sydney (latitude 33.86°S and longitude 151.21°E) is considered as the case study [17]. The house is oriented north, fully exposed to solar insolation and has a floor area of 201.2 m<sup>2</sup>. The North/South and the East/West facing walls are also 56 m<sup>2</sup> and 28.2 m<sup>2</sup>, respectively. All sides of the house are equipped with double-glazed windows to the outside environment with areas of 15 m<sup>2</sup> and 7 m<sup>2</sup> on the North and the South sides, and 4 m<sup>2</sup> on the East/West sides, respectively. All window areas include 10% of window frame areas and no blinds or shading devices associated with them. Both the walls and the flat roof of the house are comprised of the same structural insulated panels with  $R$ -value of 6.25. The floor structure is also shown in Fig. 3. All the controllable devices and schedulable loads mentioned in Section III are also implemented and included

TABLE I  
PARAMETERS USED IN COMPUTER SIMULATIONS

House Thermo-Electrical Specifications and Parameters					
Param.	Value	Unit	Param.	Value	Unit
$P_{\text{House}}^{\text{max}}$	5.5	kW	$h_o$	17	W/m <sup>2</sup> .°C
$P_{\text{grid, max}}$	±5.5	kW	$m_p, m_a$	2300, 1.198	Kg/m <sup>3</sup>
$\varepsilon, \alpha_s$	27, 73	%	$c_{p, f}, c_{p, a}$	0.88, 1.02	kJ/kg.°C
$\alpha_f$	53.7	%	$A_f$	1.2	m <sup>2</sup>
FC-based micro-CHP unit parameters					
$P_{\text{CHP, min}}^e$	0.3	kW	$P_{\text{aux, min}}^{\text{th}}$	4	kW
$P_{\text{CHP, max}}^e$	1.5	kW	$P_{\text{aux, max}}^{\text{th}}$	19	kW
$P_{\text{CHP, ramp}}^e$	0.9	kW/h	$G_{\text{ref}}$	92.4 × 10 <sup>-3</sup>	m <sup>3</sup> /h
$\eta_e, \eta_{\text{th}}, \eta_{\text{aux}}$	30, 70, 86	%	$S_{\text{CHP}}$	8	¢/start
Hot water Storage Tank specifications					
$A_{\text{st}}$	1.99	m <sup>2</sup>	$V_{\text{tot}}$	200	Liter
$R_{\text{st}}$	2.818	m <sup>2</sup> .°C/W	$T_{\text{st, min}}$	60	°C
$C_w$	0.00117	kWh/Lit.°C	$T_{\text{st, max}}$	80	°C
			$T_{\text{cw}}$	10	°C
Under Floor Heating and Cooling System Specifications					
$P_{\text{HCS, max}}$	2	kW	$\eta_{\text{H, min}}$	100	%
$t_c, t_H$	10, 40	°C	$\eta_{\text{H, max}}$	400	%
$\Delta t_{\text{CO}}, \Delta t_{\text{HO}}$	+40, -10	°C	$\eta_{\text{C, min}}$	100	%
$\Delta T_{\text{ther}}$	hot weather condition		$\eta_{\text{C, max}}$	300	%
	cold weather condition		$T_{\text{set}}$	25	°C
				±3	°C
				±2	°C
Energy Storage Device specifications					
$E_{\text{Batt}}$	24	KWh	$\text{SOC}$	20 - 80	%
$P_{\text{ch/dch, max}}$	3.3	KWh	$\eta_{\text{ch}}, \eta_{\text{dch}}$	87, 90	%

TABLE II  
SCHEDULABLE TASKS PARAMETERS

Appliance	UTR	PTR	LOT	EEC	$W$
Washing Machine	7:00-21:00	8:00-14:00	2	1	1
Dishwasher	6:00-18:00	14:00-18:00	2	1.4	2
Clothes Dryer	9:00-21:00	11:00-17:00	1	1.8	1
Iron	1:00-13:00	5:00-7:00	1	1.1	2
Vacuum Cleaner	8:00-20:00	9:00-12:00	1	0.65	2
Microwave	8:00-19:00	11:00-14:00	1	0.9	3
Rice Cooker	10:00-18:00	14:00-17:00	2	0.6	3
Electric Kettle	4:00-12:00	06:00-07:00	1	1	3
Toaster	1:00-10:00	6:00-8:00	1	0.8	3

in the experimental house using the parameters shown in Tables I and II, respectively.

Similarly, the hourly electrical power consumption of the house along with the hot water demand is shown in Fig. 4. In the same figure, the two-period moving average trend-line of the electrical demand is presented for better understanding of the user's consumption behavior, as well.

To include both the heating and cooling cases, two different simulations regarding cold and hot weather conditions are also executed with the same scenario but with different external parameters such as outdoor/basement temperatures, solar radiations, and real-time utility electricity prices, as shown in Figs. 5 and 6, respectively. It is noteworthy that the natural gas price is assumed to be 33 ¢/m<sup>3</sup> all year round [18].

Moreover, we compare the performance of the proposed algorithm through three different controlling scenarios: naive, normal, and smart. The naive scenario describes a situation in which the household does not possess or run a HAEMS; therefore there is no ability for responding to the RTP and managing

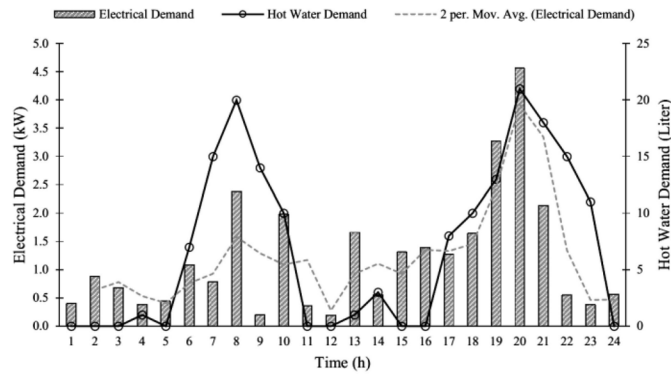


Fig. 4. Total electrical and hot water demands.

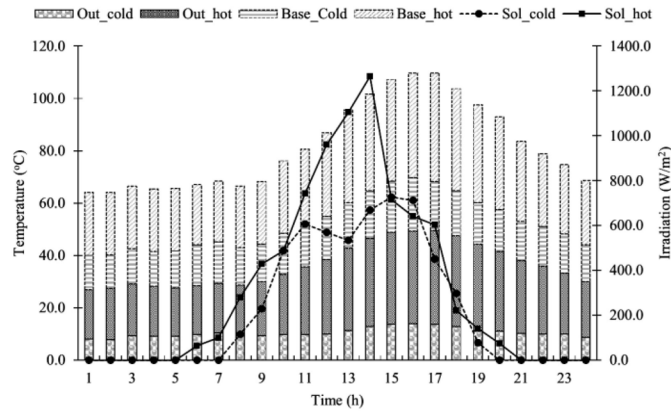


Fig. 5. Weather observations for the Sydney area [19].

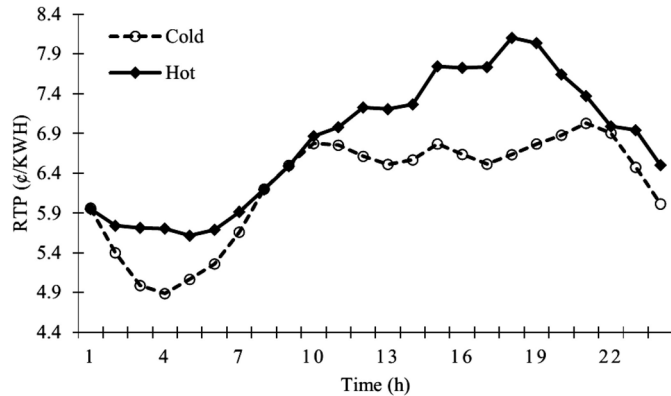


Fig. 6. Real-time utility electricity price [20].

the controllable devices according to different objectives. The tasks are executed upon the user's requests and the indoor temperature is maintained within the thermal comfort zone.

The normal controller gets real-time price signal and determines the tasks scheduling in a cost-effective way under RTP changes; however, user's preference is not considered as an objective. It also tries to maintain the house within the comfortable temperature ranges.

Unlike the previous models, the smart controller benefits from a fully-featured HAEMS and solves the optimization problem over the whole experiment duration. The controller not only reduces the domestic energy use, but also ensures an optimal task scheduling and a thermal comfort zone for

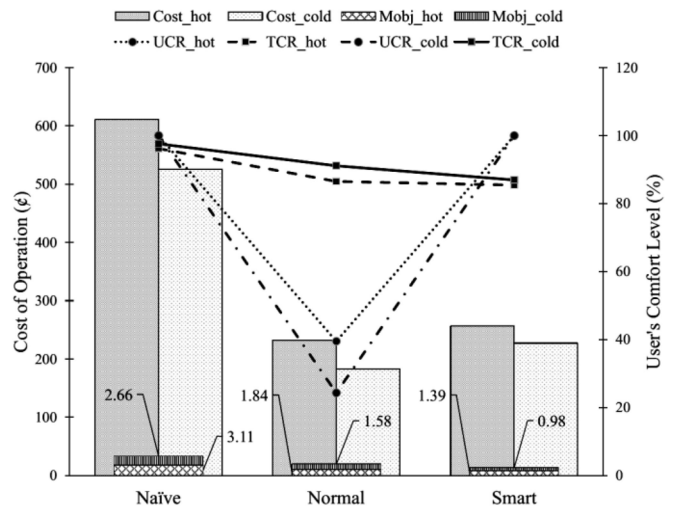


Fig. 7. Controllers' performances for the examined cooling/heating scenarios.

TABLE III  
CALCULATION TIMES OF THE CONTROLLING ALGORITHMS  
UNDER DIFFERENT SCENARIOS

Algorithm	Calculation Time (Sec.)	
	Hot Weather Conditions	Cold Weather Conditions
Naïve	1.538	1.114
Normal	2.749	2.032
Smart	4,049	3,365

the inhabitants under different system and user's imposed constraints. It should be mentioned that all of the algorithms and simulations were carried out on a PC with an Intel i5-2430M chip running Windows 7 (64-bit) with GAMS and Cplex/Dicopt solvers. Since GAMS is a high-level modeling system designed for solving linear, nonlinear, and mixed-integer optimization problems, it is selected as the main optimization engine. Also, Cplex/Dicopt solvers are utilized to allow users to combine the high level modeling capabilities of GAMS with the power of such optimizers. These solvers basically designed to solve large and difficult problems quickly and with minimal user intervention. Moreover, the mentioned solvers could automatically calculate and set most options at the best values for specific problems.

The controllers' performances are plotted in Fig. 7 for each of the examined cooling/heating scenarios. The required computational times for the mentioned algorithms are reported in Table III as well.

As observed from the simulations results, the smart controller demonstrates superior performance in comparison with the other controllers taking into account the three mentioned objectives in both scenarios. It has improved the mixed objective function value (Mobj) up to 55% and 25% with respect to the naïve and normal controllers in a hot weather condition and up to 63% and 38% in a cold weather condition. It can be also seen that the performances of the normal and smart controllers get quite close to each other in terms of cost reduction, and they produce significant energy savings compared to the naïve controller. Although the performances of the three controllers are quite competitive to each other in maintaining

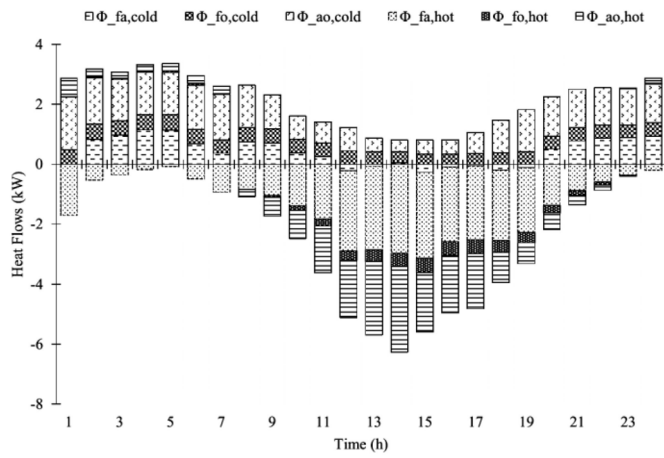


Fig. 8. Heat flows through different paths for the examined cooling/heating scenarios.

a thermal comfort zone [ $TCR = (TCL/TCL_{max}) \times 100$ ], the normal controller fails to fully satisfy the user's task scheduling needs in terms of the UCR index [ $UCR = (UCV/UCV_{max}) \times 100$ ]. From the same figure it can be observed that the controllers' performances are not the same in heating and cooling scenarios mainly due to the sun effects on the peak cooling load of a building. As shown in Fig. 8, in a hot weather condition, not only the solar heat enters the house directly through the glazing, but also the heat transfers from the exposed side of the building (including walls and the roof) to the indoor environment, which in turn increases the indoor temperature and decreases the cooling capacity of the system. It is also noteworthy that the running times of the above mentioned algorithms under different operating conditions are less than 5 s in worst cases, which are indeed small values in comparison with the typical 1-h time resolution of the simulated scenarios.

To get better insights about the smart controller performances, the optimal operation of the household devices, FC-based micro-CHP unit, and battery along with the amount of power exchange between the house and the utility are also shown in Fig. 9 for the given demand profiles in a typical hot weather condition. Likewise, the optimal operations of the heating systems with regard to the thermal demand and user's comfort level are shown in Fig. 10 for two different scenarios including the case in which, a detailed thermal model (DTM) is incorporated and the one without a detailed model (NDTM).

As it can be seen in Fig. 9, during some periods of time when the real-time electricity prices are relatively low (e.g., 3:00–7:00 and 13:00–15:00), most of the residential load is supplied by the utility; and the charging process of the battery is done with lower costs. With the growth of demand and bids of the utility during the other hours of the day, in-home units including the CHP and the battery, not only generate electricity in a cost-effective way to meet the load, but also sell the surplus of energy to the utility and make profits. Besides, optimal scheduling of household devices is done effectively regarding to associated operational constraints and user's preferences. As an example, for two consecutive tasks such as washing machine and clothes dryer, although the latter must run shortly after the former, its operation is delayed for one

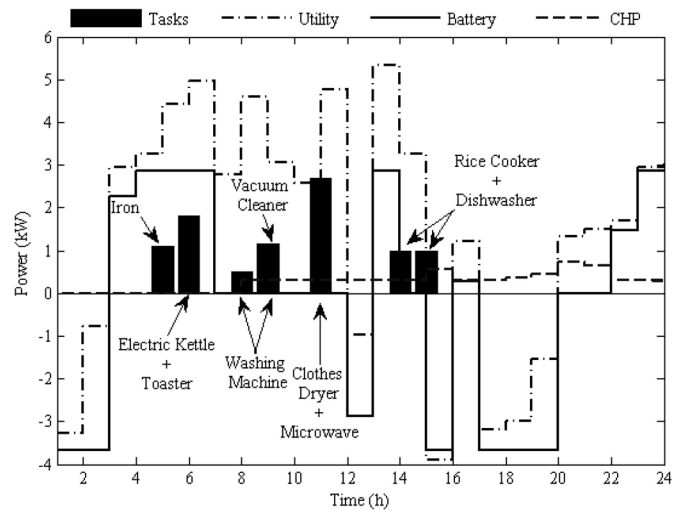


Fig. 9. Optimal operation management of devices and units.

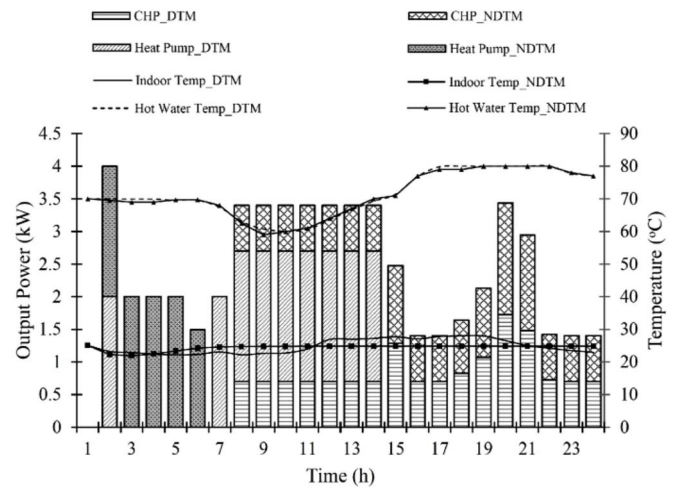


Fig. 10. Optimal operations of heating systems based on the thermal demand and user's comfort level.

hour considering the maximum allowed time gap between the operations ( $\Delta_{i,j} = 2$  h) and user's preferences.

Similarly, as observed in Fig. 10, although the smart controller maintains the indoor and the hot water temperatures within the acceptable ranges through optimal controlling of underfloor heating/cooling system and the micro-CHP unit, there exist some differences between the operation of the mentioned systems under DTM and NDTM scenarios. Regarding to a DTM, the heat pump is run more to handle more heat between the indoor and the outdoor environment for the body comfort while in a NDTM there is no need for frequent operation of the heating/cooling system. Likewise, the variation of the indoor temperature within the acceptable range is clearly observed in a DTM due to the heat flows between the indoor node and the external environment, such as walls, roof, and the sky, but such a variation is not noticeable in case of NDTM. On the other hand, the operation of CHP unit and the temperature of hot water are slightly different in these scenarios because the heat loss of the storage tank is not considerable in both cases.

## V. CONCLUSION

In this paper, a multiobjective MINLP-based smart energy management system for residential scenarios has been described and valued through different operating conditions. The proposed model, which benefits from a fully-featured HAEMS, could schedule household devices and micro-sources optimally taking into account a meaningful balance between the energy saving and a comfortable lifestyle.

It was demonstrated (through simulation case studies) that under different system and users imposed constraints the proposed algorithm could not only reduce the domestic energy use, but also ensured an optimal task scheduling and a thermal comfort zone for the inhabitants. To verify the efficiency and robustness of the proposed model, a number of simulations were also performed under different heating/cooling scenarios with real data and the obtained results were compared with those from conventional models in terms of total operation cost, user's convenience rate, and TCL.

Future efforts will be mainly aimed at improving the optimization framework by taking into account more real smart-home settings and environments. This will allow us to scrutinize how closely real conditions can be modeled with uncertain parameters and random processes. We also need to further investigate how different user's preferences or pricing schemes (such as flat rate and time of use) influence the performance of the proposed algorithm. We will also conduct more experiments on larger test systems such as a residential micro-grid with multiple small or medium size houses and investigate the effectiveness of our proposed architecture in a multiagent based simulation environment.

## REFERENCES

- [1] M. Ali, J. Jokisalo, K. Siren, and M. Lehtonen, "Combining the demand response of direct electric space heating and partial thermal storage using LP optimization," *Elect. Power Syst. Res.*, vol. 106, pp. 160–167, Jan. 2014.
- [2] A. Molderink, V. Bakker, M. Bosman, J. Hurink, and G. Smit, "Domestic energy management methodology for optimizing efficiency in smart grids," in *Proc. IEEE Conf. Power Technol.*, Bucharest, Romania, Jun. 2009, pp. 1–7.
- [3] A.-H. Mohsenian-Rad and A. Leon-Garcia, "Optimal residential load control with price prediction in real-time electricity pricing environments," *IEEE Trans. Smart Grid*, vol. 1, no. 2, pp. 120–133, Sep. 2010.
- [4] A.-H. Mohsenian-Rad, V. W. Wong, J. Jatskevich, R. Schober, and A. Leon-Garcia, "Autonomous demand-side management based on game-theoretic energy consumption scheduling for the future smart grid," *IEEE Trans. Smart Grid*, vol. 1, no. 3, pp. 320–331, Dec. 2010.
- [5] A. Barbato *et al.*, "House energy demand optimization in single and multi-user scenarios," in *Proc. IEEE Int. Conf. Smart Grid Commun.*, Brussels, Belgium, Oct. 2011, pp. 345–350.
- [6] P. Du and N. Lu, "Appliance commitment for household load scheduling," *IEEE Trans. Smart Grid*, vol. 2, no. 2, pp. 411–419, Jun. 2011.
- [7] M. Tasdighi, H. Ghasemi, and A. Rahimi-Kian, "Residential microgrid scheduling based on smart meters data and temperature dependent thermal load modeling," *IEEE Trans. Smart Grid*, vol. 5, no. 1, pp. 349–357, Jan. 2014.
- [8] F. de Angelis *et al.*, "Optimal home energy management under dynamic electrical and thermal constraints," *IEEE Trans. Ind. Informat.*, vol. 9, no. 3, pp. 1518–1527, Aug. 2013.
- [9] N. Gudi, L. Wang, V. Devabhaktuni, and S. S. R. Depuru, "Demand response simulation implementing heuristic optimization for home energy management," in *Proc. N. Amer. Power Symp.*, Arlington, TX, USA, Sep. 2010, pp. 1–6.
- [10] T. Huang and D. Liu, "A self-learning scheme for residential energy system control and management," *Neural Comput. Appl.*, vol. 22, no. 2, pp. 259–269, Feb. 2013.

- [11] D. Fuselli *et al.*, "Optimal battery management with ADHDP in smart home environments," in *Advances in Neural Networks*, vol. 7368. Berlin, Germany: Springer-Verlag, 2012, pp. 355–364.
- [12] H. Morais, P. Kádár, P. Faria, Z. A. Vale, and H. M. Khodr, "Optimal scheduling of a renewable micro-grid in an isolated load area using mixed-integer linear programming," *Renew. Energy*, vol. 35, no. 1, pp. 151–156, 2009.
- [13] D. M. Han and J. H. Lim, "Smart home energy management system using IEEE 802.15.4 and ZigBee," *IEEE Trans. Consum. Electron.*, vol. 56, no. 3, pp. 1403–1410, Aug. 2010.
- [14] *ASHRAE Handbook-Fundamentals*, American Society of Heating, Refrigerating and Air-Conditioning Engineers, Atlanta, GA, USA, 2001.
- [15] P. Scott, S. Thiebaut, M. van den Briel, and P. van Hentenryck, "Residential demand response under uncertainty," in *Proc. Int. Conf. Princ. Pract. Constraint Program. (CP)*, Uppsala, Sweden, Sep. 2013, pp. 645–660.
- [16] J. Wang, S. Kennedy, and J. Kirtley, "A new wholesale bidding mechanism for enhanced demand response in smart grids," in *Proc. Innov. Smart Grid Technol. (ISGT)*, Gaithersburg, MD, USA, 2010, pp. 1–8.
- [17] S. M. Bambrook, A. B. Sproul, and D. Jacob, "Design optimization for a low energy home in Sydney," *Energy Build.*, vol. 43, no. 7, pp. 1702–1711, 2011.
- [18] (2013, Oct. 15). *Compressed Natural Gas (CNG) Systems* [Online]. Available: <http://www.oes.net.au>
- [19] (2013, Sep. 28). *Climate Data Online* [Online]. Available: <http://www.bom.gov.au>
- [20] (2013, Sep. 28). *Electricity Price & Demand* [Online]. Available: <http://www.aemo.com.au>



**Amjad Anvari-Moghaddam** (GSM'08) received the B.S. (Hons.) degree from the Ferdowsi University of Mashhad, Mashhad, Iran, in 2008, and the M.Sc. (Hons.) degree from Shiraz University, Shiraz, Iran, in 2010, both in electrical engineering. He is currently pursuing the Ph.D. degree in electrical engineering from the University of Tehran (UT), Tehran, Iran.

He is currently a Research Assistant with UT. His current research interests include smart micro grids (SMGs), renewable energies and multiagent systems design, and operation and control.



**Hassan Monsef** received the B.Sc. degree from the Sharif University of Technology, Tehran, Iran, in 1986; the M.Sc. degree (Hons.) from the University of Tehran (UT), Tehran, in 1989; and the Ph.D. degree from the Sharif University of Technology, in 1996, all in power engineering.

He has been with the School of Electrical and Computer Engineering, University College of Engineering, UT, since 1996, where he is currently an Associate Professor. His current research interests include power system operation under deregulation, reliability of power system, power systems economics, and renewable energy systems and its integration in smart grid.



**Ashkan Rahimi-Kian** (SM'08) received the B.Sc. degree from the University of Tehran, Tehran, Iran, in 1992, and the M.S. and Ph.D. degrees from Ohio State University, Columbus, OH, USA, in 1998 and 2001, respectively, all in electrical engineering.

He was the Vice President of the Engineering and Development Department with Genscape, Inc., Louisville, KY, USA, from 2001 to 2002, and was a Research Associate with the School of Electrical and Computer Engineering (ECE), Cornell University, Ithaca, NY, USA, from 2002 to 2003. He is currently an Associate Professor in the Electrical Engineering Department (Control and Intelligent Processing Center of Excellence) with the School of ECE, College of Engineering, University of Tehran (UT), Tehran. He is also the Founder and Director of the Smart Networks Research Laboratory with the School of ECE, UT. His current research interests include bidding strategies in dynamic energy markets, game theory and learning, intelligent transportation systems, decision making in multiagent stochastic systems, stochastic optimal control, dynamic stock market modeling and decision making using game theory, smart grid design, operation and control, estimation theory and applications in energy and financial systems, risk modeling, and management in energy and financial systems.